Pattern formation in the flow between two horizontal coaxial cylinders with a partially filled gap

Innocent Mutabazi,* John J. Hegseth, and C. David Andereck
Department of Physics, Ohio State University, 174 West 18th Avenue, Columbus, Ohio 43210

Jose E. Wesfreid
Laboratoire d'Hydrodynamique et Mécanique Physique, Ecole Supérieure de Physique et de Chimie Industrielles de la Ville de Paris, 10 rue Vauquelin, 75231 Paris Cédex 05, France

(Received 29 February 1988)

Flow between two horizontal coaxial cylinders with a partially filled gap is subject to several types of centrifugal instabilities which lead to the formation of a variety of spatial patterns. An experimental investigation has shown that there are five distinct branches of primary instabilities occurring in the system and that four codimension-2 points are easily reached. Theoretical predictions are in qualitative agreement with the observations.

I. INTRODUCTION

The behavior of systems far from equilibrium has been the subject of intense investigation over the last several years. Of particular interest has been the manner in which spatial patterns arise. Pattern formation may be driven by a wide variety of mechanisms, including temperature gradients, concentration gradients, and centrifugal effects. Centrifugal instabilities[1,2] occur in flow with curved streamlines, and they play an important role in many problems of practical importance. Two of the best known examples are the Taylor-Couette instabilities, which occur in the flow between two concentric rotating cylinders, and the Taylor-Gortler instabilities, which occur in the boundary layer on a concave wall. The Taylor-Couette and Taylor-Gortler instabilities have been extensively investigated both theoretically and experimentally (see Refs. 3–5 and references therein). However, a third class, the Dean instabilities,[6] which occur in the presence of a pressure gradient along a curved channel (Poiseuille flow), has received much less attention.

Here, we present a simple system in which it is possible to realize the main centrifugal instabilities by an appropriate choice of control parameters. We consider two horizontal coaxial cylinders of radii r_i and r_o, which rotate independently with angular velocities Ω_i and Ω_o for the inner and the outer cylinder, respectively. When the gap between the cylinders is completely filled with fluid, we have the classical Taylor-Couette problem. When the gap is partially filled and both cylinders rotate there exists a combination of Taylor-Couette flow (caused by the differential rotation of the cylinders) and Poiseuille flow (caused by the backflow induced by the presence of the horizontal free surfaces). As the system control parameters are varied, the base flow instabilities will change from those associated with Taylor-Couette to those associated with Dean. Under some conditions one might expect to see flow patterns that result from competition between instabilities. In other cases boundary layers on the curved surfaces may give rise to Taylor-Gortler instabilities.[7] We will not discuss the last any further since boundary layer instabilities are apparently not dominant for the range of system parameters chosen. The relevant control parameters are the ratio of angular velocities $\mu=\Omega_o/\Omega_i$ and the Taylor number.

In Sec. II we will summarize the few related experimental and theoretical results which have been reported so far. In Sec. III we describe our experimental procedure and in Sec. IV we report the results obtained. Section V is a comparison of the experimental results with the present theory. Finally, we will conclude with suggested directions for future work.

II. PREVIOUS WORK

The flow between two horizontal coaxial cylinders with a partially filled gap was first investigated by Brewster and Nissan[8] in 1958. They deduced approximate velocity fields for laminar flow with only the inner cylinder rotating, and they measured the critical angular velocity and the wave number of the resulting rolls. In 1959, Brewster, Grosberg, and Nissan[9] considered the critical conditions for the formation of vortices between the cylinders in three cases: when the gap is filled with fluid and the flow is caused by the rotation of the inner cylinder (Taylor-Couette problem), when the flow is produced by pumping around the annular space (Dean problem), and when the liquid is driven by the rotation of the inner cylinder and forced to reverse its flow at a free surface. Their results for the Dean problem were in satisfactory agreement with the theoretical values for the threshold of the instability and the wave number of the vortices. They considered also the combination of the pumping of fluid around the annular space and the rotation of the inner cylinder. They obtained the interesting result that, in the neighborhood of a particular value of the ratio of the pumping flow rate to the rotation flow rate, the critical value of the control parameter has an abrupt change, and

the wavelength of the vortices has a discontinuity. The competition between the destabilization of the Couette and Poiseuille layers in the basic flow was invoked to explain this anomalous behavior.

DiPrima,[10] using a Galerkin method, calculated the stability diagram for the combined Couette-Poiseuille problem and introduced a parameter λ which measures the relative importance of the pumping flow compared to the flow driven by the rotation of the inner cylinder. He found that the neutral stability curve (using the principle of exchange of stabilities, which assumes that the instability that occurs is stationary) exhibits a discontinuity for $\lambda=\lambda_c=-3.667$. Hughes and Reid[11] found, by numerically integrating the stability equations, that, in the vicinity of λ_c, the marginal stability curve presents two minima with different values of wave numbers. Raney and Chang[12] relaxed the restrictions of the principle of exchange of stabilities and found that, in the vicinity of λ_c, the marginal stability curve consisted of two stationary loops connected by an oscillatory branch at the absolute minimum of the control parameter. They came to the conclusion that in the neighborhood of λ_c, an oscillatory instability might occur. No experimental verification of this result has been reported so far, perhaps because of the difficulty of realizing a well-controlled flow with external pumping.

Mutabazi, Peerhossaini, and Wesfreid[7] have reported experimental results for the case of a partially filled gap with only the inner cylinder rotating. They emphasized the oscillatory character of the observed structures and found a lower value of the threshold of instability than that claimed by Brewster and Nissan.[8] In another paper Mutabazi *et al.*,[13] describe the quantitative characteristics of the oscillatory structures. Recently, Mutabazi, Normand, Peerhossaini, and Wesfreid[14] have solved the linear stability problem for axisymmetric perturbations in the flow between two co-rotating cylinders with a partially filled gap. They found that at the instability threshold in such a system it is possible to detect oscillatory or stationary rolls depending on the ratio of the angular velocities μ. The intersection points (codimension-2 points) of the oscillatory and stationary branches in the diagram (μ, T_c), where T_c is the critical value of the Taylor number considered as the control parameter of the flow, were predicted to be experimentally accessible. We report here the results of an initial test of these predictions.

III. EXPERIMENTAL PARAMETERS AND PROCEDURES

The system considered in our experiment has been previously used in the investigation of Taylor-Couette instabilities and is described in Baxter and Andereck.[15] It consists of two horizontal coaxial cylinders, the inner one made of black Delrin plastic (radius $r_i=5.262$ cm) and the outer one made of polished Plexiglas (radius $r_o=5.965$ cm). So the radius ratio $\eta=0.882$ and the gap is given by $d=r_o-r_i=0.703$ cm. Teflon rings attached to the outer cylinder define the left and right boundaries for the liquid and produce an aspect ratio (working space length/gap) $\Gamma=68$. The cylinders were driven by Compumotor stepping motors with a rotation-rate resolution of 0.001 Hz. The angular velocities Ω_i and Ω_o of the inner and outer cylinders are scaled in terms of Reynolds numbers $R_i=\Omega_i r_i d/\nu$ and $R_o=\Omega_o r_o d/\nu$, where ν is the kinematic viscosity of the working fluid. As shown in Fig. 1, the gap is filled only about $\frac{2}{3}$ full with distilled water to avoid communication between the two sides of the system. The rotation of the cylinders typically induces no significant film on the walls. The experiments were performed in a controlled environment room; the fluid temperature varied by no more than 0.1 °C. Visualization of the flow states has been accomplished with a mixture of 1% by volume Kalliroscope AQ1000 in water. Interpretation of structures observed in the flow with polymeric flakes is based on the following: a dark area indicates flow along the observer's line of sight, while a light area indicates flow perpendicular to the line of sight. However, the asymmetry between the radial inflow and outflow boundaries can produce confusion between the wavelength and roll size of patterns if one boundary is much less distinct than the other.

Data acquisition involved two techniques. Flow frequencies were determined from a single point time series obtained with laser light reflected off the Kalliroscope flakes onto a photodiode detector. The resulting signal was digitized for processing with a fast Fourier transform (FFT) routine. Spatial data were obtained by eye and by using a 28–85-mm variable focal length lens to form an image of the visualized flow on a 1024-pixel charge-coupled device (CCD) linear array interfaced through CAMAC to the computer. The line of 1024 pixels is oriented parallel to the cylinder axis. The output consists of intensity maxima and minima which correspond to the centers of the rolls and inflow and outflow boundaries, respectively. Analysis of the intensity plots yields the vortex sizes and hence the wavelength of the structure.

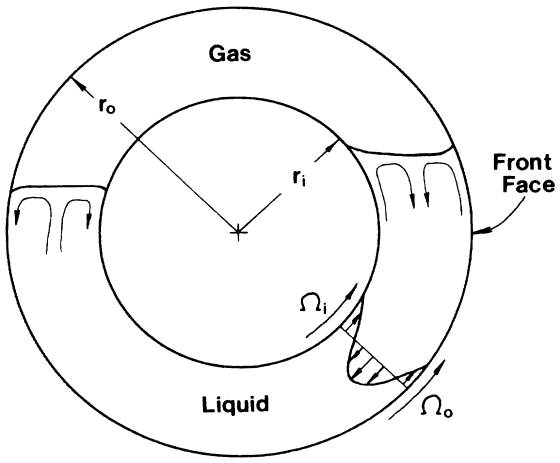

FIG. 1. Schematic cross section of the apparatus. The "front face" is defined to mean that the observer sees the inner cylinder rotating upward as shown. The outer cylinder can rotate in either direction. Qualitative pictures of the flow near the free surfaces are shown, along with the fully developed velocity profile away from these surfaces.

IV. RESULTS

The transitions from unperturbed flow to the various critical states are summarized in Fig. 2. The observations were made from the front face (as defined in Fig. 1), while the rear face was viewed simultaneously, when needed, by a video camera and monitor. The system control parameters are the Reynolds numbers R_i and R_o (defined above), respectively, for the inner and the outer cylinders [the base flow may also be specified by the angular velocities ratio μ and the Taylor number defined as $T=(\Omega_i r_i d/\nu)(d/r_i)^{1/2}$ but the first pair of parameters has the advantage of being more easily controlled in an experiment]. For our experiments the two sets of parameters are related as follows: $\mu=0.882R_o/R_i$ and $T=0.366R_i$ (or $R_i=2.736T$ and $R_o=3.102\mu T$). In presenting our results we will scale wavelengths by d, velocities by ν/d, and frequencies by ν/d^2.

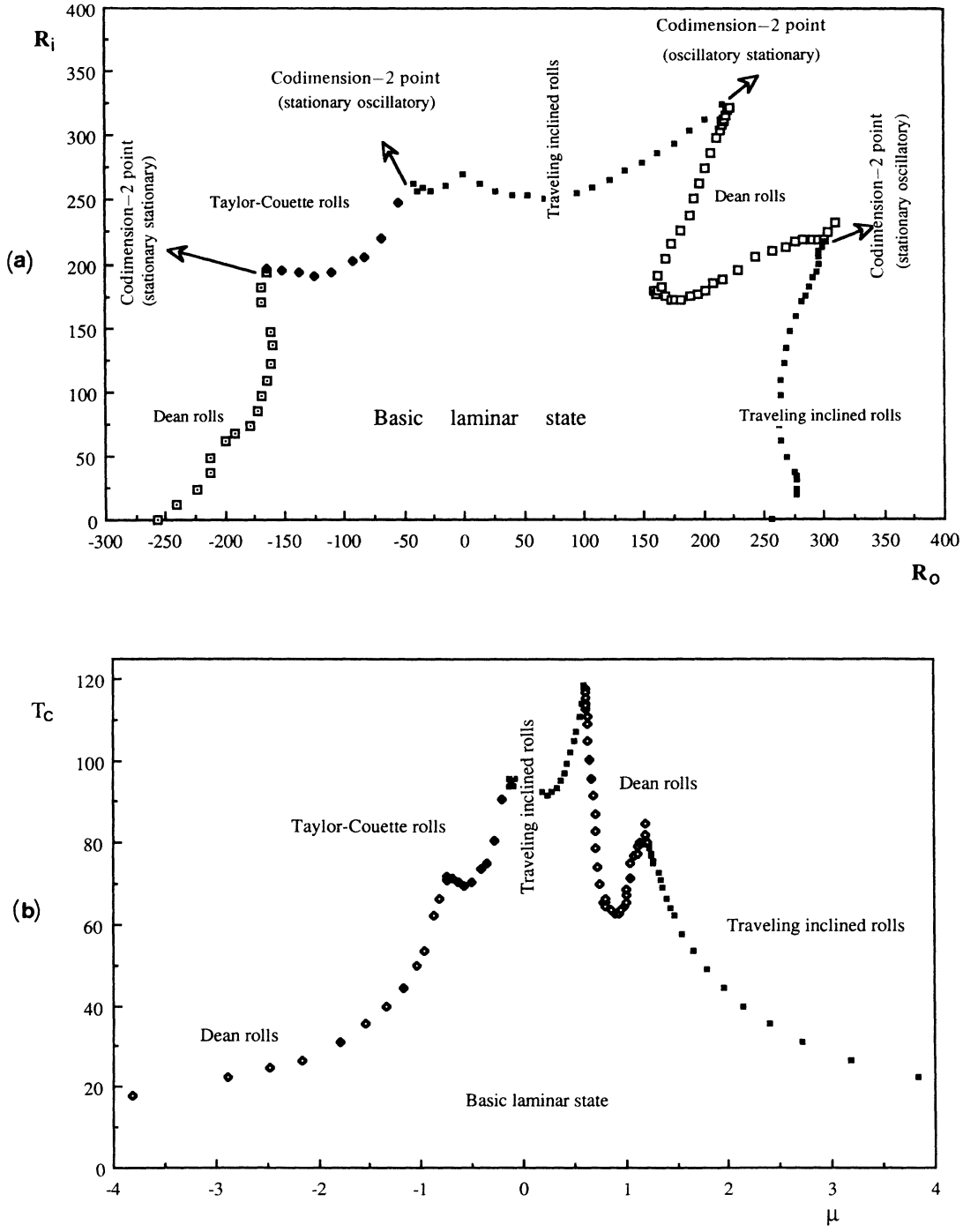

FIG. 2. (a) Diagram of primary flow transitions in the (R_0, R_i) space. (b) Diagram of primary flow transitions in the (μ, T) space.

A. Base flow

The fully developed base flow between two infinite horizontal coaxial cylinders with a partially filled gap is azimuthal (except in the neighborhood of the free surfaces) if the entrance angle θ_e is small compared to the filling angle $\theta_f (\approx 4\pi/3$ for our experiment). The entrance angle is given, for $\mu=0$, by[13] $\theta_e=\Omega_i d^2/9\pi^2\nu=2f_i/9\pi$, where f_i is the scaled frequency of rotation of the inner cylinder. Then the condition for assuming fully developed azimuthal base flow is $f_i \ll f_o=9\pi\theta_f/2$. For our experimental case $f_o=67.1$. We have worked in the range $0.5 \le f_i \le 15.5$, with $f_c \le 7.2$ for all the transitions. At these rotation frequencies we can consider our base flow to be essentially azimuthal. The azimuthal velocity profile is given by[16] $V(r)=Ar\ln r+Br+C/r$, where $A=(1/2\rho\nu)\partial P/\partial\theta$ is related to the azimuthal pressure gradient and the coefficients B and C are obtained from the boundary conditions on the cylindrical walls. The flow rate conservation across a given radial section (θ=constant plane) gives the value of A. We get

$$A=\frac{2[2(\Omega_i-\Omega_o)r_i^2r_o^2\ln(r_o/r_i)+(\Omega_o r_o^2-\Omega_i r_i^2)(r_o^2-r_i^2)]}{(r_o^2-r_i^2)^2-4r_i^2r_o^2[\ln(r_o/r_i)]^2}, \tag{1}$$

$$B=\frac{(\Omega_o r_o^2-\Omega_i r_i^2)-A(r_o^2\ln r_o-r_i^2\ln r_i)}{r_o^2-r_i^2}, \tag{2}$$

$$C=\frac{[\Omega_i-\Omega_o+A\ln(r_o/r_i)]r_i^2r_o^2}{r_o^2-r_i^2}. \tag{3}$$

The coefficient A in $V(r)$ is zero in the classical Couette problem (fully filled gap). The velocity profile is a superposition of the Couette flow imposed by the rotation and the Poiseuille flow in a curved channel produced by the azimuthal pressure gradient. This superposition is well seen in the small-gap approximation. For the purposes of our experiment, we will use the small-gap approximation ($\eta\to 1$) and introduce a characteristic velocity ν/d to obtain the quadratic trinomial in x [with $x=(r-r_i)/d$]:

$$V(x)=3(R_i+R_o)x^2-2(2R_i+R_o)x+R_i. \tag{4}$$

This profile possesses up to two nodal surfaces (surfaces of zero azimuthal velocity) between the two cylinders situated at

$$x=\frac{2R_i+R_o\pm\sqrt{R_i^2+R_iR_o+R_o^2}}{3(R_i+R_o)}. \tag{5}$$

Figure 3 gives the velocity profiles for different values of the parameters R_i and R_o. Examination of these base flows reveals the possibility for centrifugal instabilities. To a first approximation the centrifugally unstable regions will be those in which the inviscid Rayleigh circulation criterion ($d/dr\,|\,\Omega r^2\,|<0$) holds, as noted in the figure. The presence of viscosity modifies this simple picture, but the basic instabilities remain. These have been examined numerically by Mutabazi *et al.*[14]

B. Stationary patterns

For R_o in the ranges of -257–-35 and 160–257, the base flow is typically unstable to formation of a pattern of time-independent vortices. (The behavior near $R_i=0$ is rather different and will be discussed at length in Sec. IV E.) They have no significant azimuthal variation, except very near the free surfaces, and are of uniform size along the cylinder, with a dimensionless wavelength of the vortex pairs (defined as λ/d) of about 2.4 in the corotating case and approximately 2.45 in the counterrotating flows [see Figs. 4(a) and 4(b)]. The patterns for $-257<R_o<-175$ and for $160<R_o<270$ are clearly observed and therefore are most likely forming near the outer cylinder. The analysis of the approximate base flow profile suggests that these are Dean rolls.[14] For $-257\le R_o\le -170$, Rayleigh's criterion applied to the profile of Fig. 3(a) shows that the potentially unstable layer in the gap is contained within the Poiseuille flow region, which will therefore give rise to Dean rolls. For $160\le R_o\le 270$ numerical results[14] show that the rolls should be confined to the outer unstable layer, which again is part of a Poiseuille flow region, indicating these are also Dean rolls. Slightly beyond the onset of the instability, subharmonics intervene, leading to rather complex patterns.

For $-170<R_o<-35$, the rolls are difficult to observe, being apparently localized near the inner cylinder, and they do not strengthen significantly as R_i is increased. These are probably Taylor-Couette vortices [Fig. 4(c)] because the destabilized layer near the inner cylinder has a velocity profile [see Fig. 3(c)] which is Couette-like rather than Poiseuille-like. The transition between these theoretical profiles occurs near the experimental codimension-2 point at $R_i=197$ and $R_o=166$. For R_o from -175 to -170, the rolls appear first in the rear face. This branch has been explored in two ways, both by fixing R_o and changing R_i, and by fixing R_i and changing R_o, and the results were essentially the same. The Dean rolls and Taylor-Couette rolls are both unstable to time-dependent patterns (traveling inclined rolls; see Sec. IV B) when R_i is increased for fixed R_o, except, of course, for

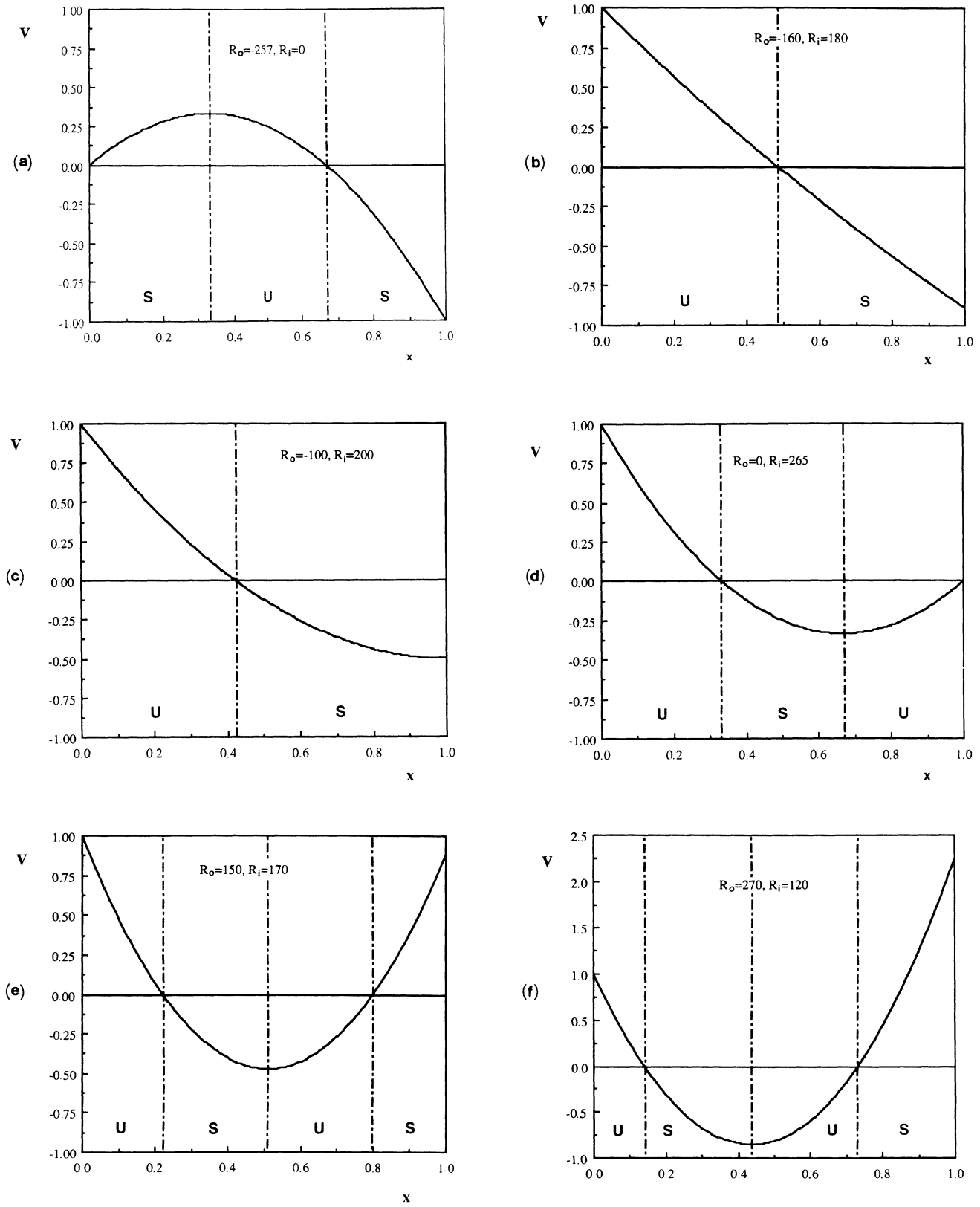

FIG. 3. Base flow velocity distributions near instability thresholds (flow patterns arising from the base flow instabilities are indicated in parentheses): (a) only outer cylinder rotating, (b) counter-rotating cylinders (Dean rolls), (c) counter-rotating cylinders (Taylor-Couette rolls), (d) only inner cylinder rotating (traveling inclined rolls), (e) co-rotating cylinders (Dean rolls), (f) co-rotating cylinders (traveling inclined rolls). *S* and *U* indicate Rayleigh stable and unstable layers, respectively. The fluid velocities have been normalized to the outer cylinder velocity in (a) and the inner cylinder velocity in (b)–(f).

R_o from 150 to 200, in which case the base flow is regained before traveling rolls form.

C. Time-dependent patterns

Traveling spirals (or, technically, traveling inclined cells, since a complete spiral is not really possible owing to the presence of the free surfaces) [Fig. 4(c)] appear at threshold for R_o in the ranges -30–210 and 265–300. They form at an angle of about 20° with the vertical and propagate along the cylinder axis with a constant velocity. The dimensionless roll propagation velocity, scaled by ν/d, is approximately 29 (0.4 cm/sec). Figure 5 shows

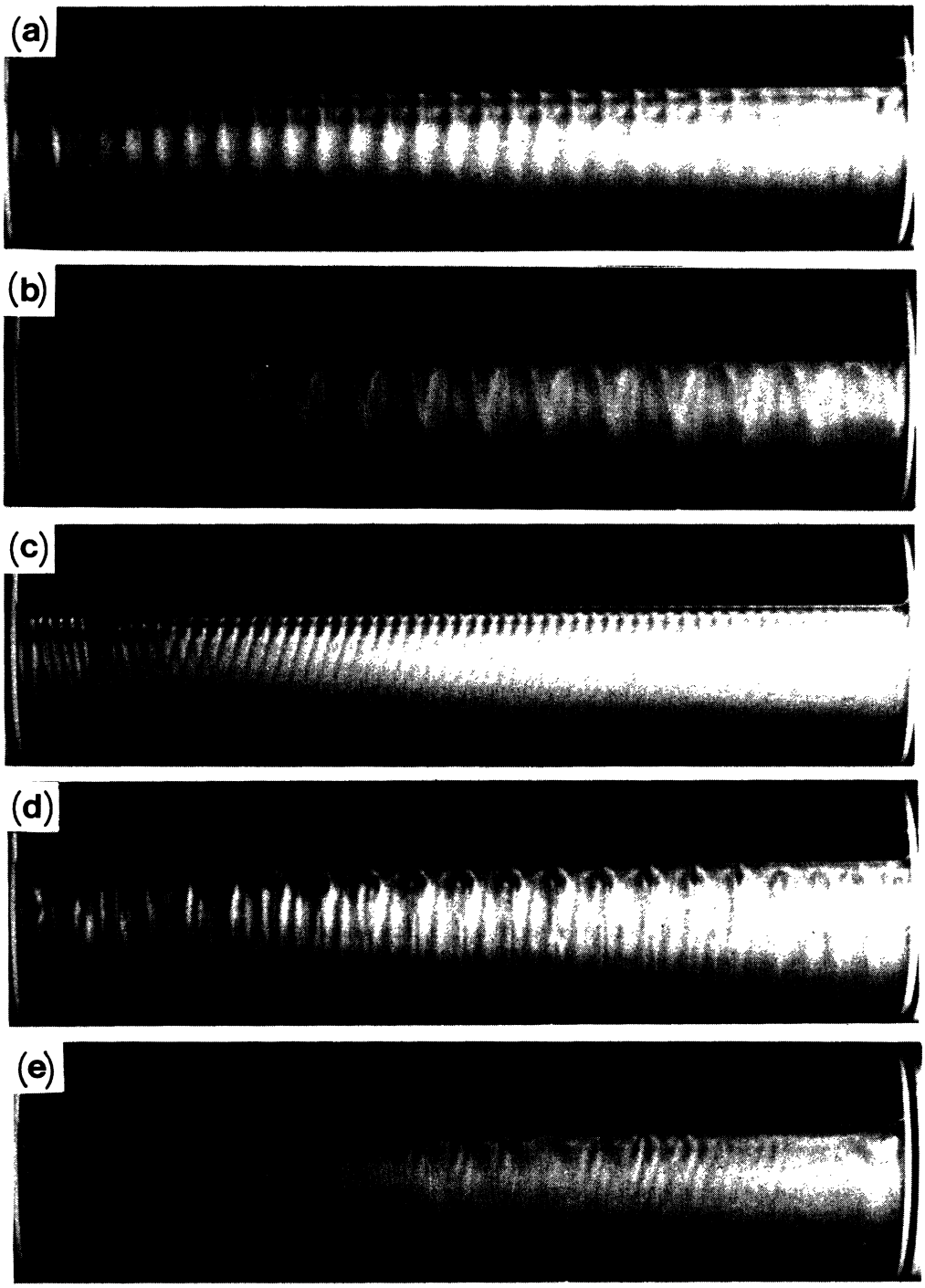

FIG. 4. States observed for different values of control parameters: (a) Dean rolls, $R_o=220$, $R_i=195$, (b) Taylor-Couette rolls, $R_o=-136$, $R_i=252$, (c) inclined traveling rolls, $R_o=70$, $R_i=280$, (d) Dean rolls for only the outer cylinder rotating, $R_o=320$, $R_i=0$, (e) coexisting inclined and Dean rolls, $R_o=-45$, $R_i=265$.

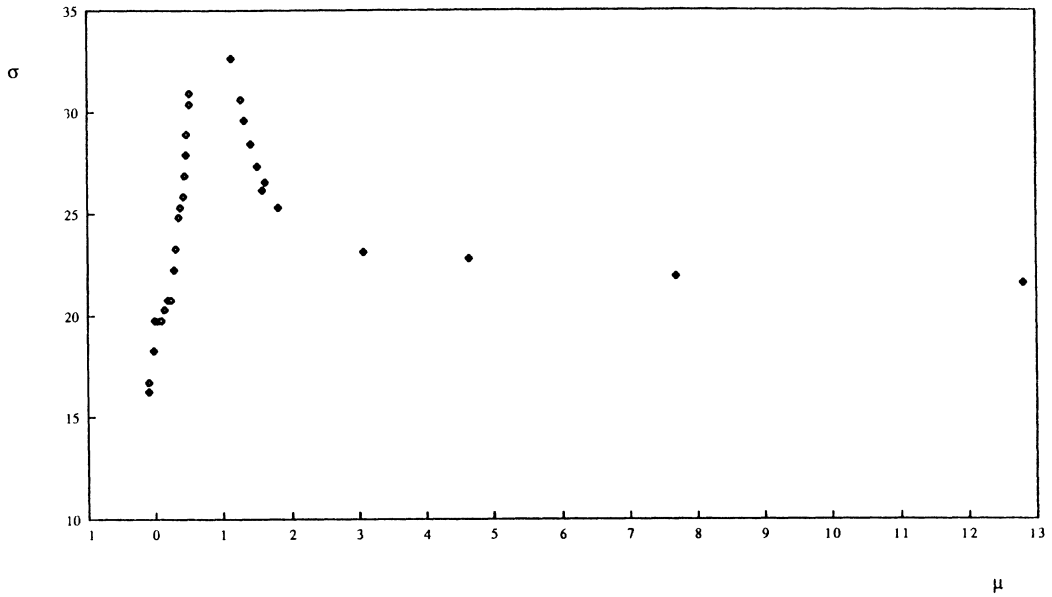

FIG. 5. The frequency σ of traveling inclined rolls vs μ the ratio of the angular velocities of the two cylinders. σ is the measured frequency in Hertz scaled by d^2/ν. The region between the two branches corresponds to the stationary patterns. The ends of the two branches correspond to the codimension-2 points.

the frequency as a function of the angular velocities ratio μ. It is interesting that there is no preferred propagation direction for the rolls; they may move from either left to right or right to left, but the relationship of the tilt direction to the direction of propagation is always the same. Occasionally there may be inclined rolls with opposite tilt and propagation direction existing simultaneously in different regions along the cylinder. Usually one will occupy almost the entire length with the other confined near one end. Although in principle standing waves formed by counterpropagating rolls may exist we have not yet observed this effect. The inclined rolls become much weaker partway around the cylinder, with greatest strength near the front face. It is possible that the presence of the free surfaces accounts for this by imposing an entrance length region on the fully developed Couette and Poiseuille profile.[7] Above threshold the rolls become clearly visible all the way from the front to the back free surface, corresponding to a decrease of the entrance length.

D. Laminar state-inclined rolls-laminar state-stationary patterns transition

There are two bands of R_o values (from 155 to 210 and from 257 to 300) for which the instability differs as R_i is increased. In the first band, when R_i is increased from about 160, the instability sets in as stationary axisymmetric rolls, but at higher R_i they disappear and the flow becomes laminar, without any structures. At still higher values of R_i inclined rolls form. In the second band the instability sets in as a traveling pattern. Upon increasing R_i the pattern disappears and the base laminar flow reappears. At still larger R_i stationary axisymmetric rolls form in the flow. The roll size is the same as that for the stationary patterns for R_o in the range 160–257. It is interesting to notice that if we plot the phase diagram [Fig. 2(a)] in terms of the parameters T and μ [Fig. 2(b)], the transition, for fixed μ and increasing T, is directly from the base state to inclined rolls or to the stationary Dean rolls.

E. Codimension-2 points

The traveling inclined roll state and the stationary state branches intersect at three oscillatory-stationary codimension-2 points. Preliminary inspections of the neighborhoods of these points have proved quite interesting. There are often mixed states of stationary and traveling rolls. Sometimes the traveling rolls are near the right end and the stationary rolls are near the left end (or vice versa), or the traveling rolls may coexist with the stationary rolls in the same region [see Fig. 4(e)]. The Dean and Taylor-Couette branches intersect in another codimension-2 point (stationary-stationary). Near that point rolls which were clearly visible at the outer cylinder wall become less distinct as the unstable region develops near the inner cylinder wall.

In all cases the system was brought to just beyond the instability threshold and then allowed to settle for many gap diffusion times d^2/ν, following which the process was repeated. It might be possible that these states near the codimension-2 points are transients: waiting for a very long time, the system may pass to a pure state like those prevailing further from the immediate neighborhood of the codimension-2 point, but this has not been established, owing to practical difficulties with Kalliroscope solution lifetime limits. Further work will be necessary to achieve a coherent picture of these complex flows.

F. Inner cylinder at rest, outer cylinder rotating

When the inner cylinder is at rest and the outer cylinder is rotating, there is some difficulty in establishing the onset of the instability. End effects dominate the flow. Large spiral-like vortices propagating away from each end virtually fill the system. They are most prominent on the side with the outer cylinder moving upward. On the other side at $R_o = 257$ weak stationary Dean rolls form and coexist with the end-effect rolls. Increasing R_o to 300 establishes Dean rolls on both sides of the system, and the end effects become less apparent [Fig. 4(d)]. It is then possible to decrease R_o to 272 and retain the axisymmetric state. After establishing Dean rolls throughout, one can then increase R_i slowly and observe various transitions. Two cases arise: when the cylinders are counter-rotating, these rolls persist but become weaker in the back face. For co-rotating cylinders, the Dean rolls are observed to be asymmetric, weaker in the front face than in the back, until $R_i \simeq 12$, at which point traveling inclined rolls appear in the front face. The transition between Dean rolls and inclined rolls in this region has not been thoroughly explored.

V. DISCUSSION OF RESULTS

The stationary states of the diagram (R_o, R_i) may be understood at least qualitatively if one applies the Rayleigh stability criterion to the base flow velocity profile. In fact, from Fig. 3, one sees that the velocity profile may be considered as a superposition of linear Couette and Poiseuille profiles. Depending on the critical Reynolds number for the different sublayers, the onset of instability for the whole system will begin in that sublayer with the minimal critical value. The inclined roll states might be understood as the result of the competition between the mechanisms of destabilization of the Couette and Poiseuille sublayers. In fact, we see in Fig. 3 that the inclined rolls exist for those values of R_i and R_o for which the base velocity field has two potentially unstable sublayers, while the stationary states develop for the case when the base velocity profile has only one potentially unstable sublayer. The Dean rolls which emerge for R_o in the range 160–300 appear to be an exception to this and they may be seen as intermediate between the inclined roll and laminar states. It is also interesting to remark that the system is always linearly unstable with either the inner or the outer cylinder at rest, while for the classical Taylor-Couette system the flow is linearly stable when the inner cylinder is at rest. The result obtained for the case with only the inner cylinder rotating agrees with the results found previously and reported in Refs. 7 and 13.

The presence of an oscillatory branch in between two distinct stationary branches has been predicted,[14] but the observed critical values were quite different from those calculated. In particular, the oscillatory branch was predicted to exist between the codimension-2 points at $R_o = 142$, $R_i = 483$ and $R_o = 216$, $R_i = 489$. (Theoretical critical values have been omitted from Fig. 2 since they are quite large compared with the experimental values.) Several assumptions were made in developing the initial theory, among which are the small gap approximation, the infinite cylinder length, and the axisymmetric perturbations (even though the system itself breaks the azimuthal symmetry). Nevertheless, the predicted frequency is of the same order as that observed in the experiment. For stationary states, axisymmetric perturbations may still suffice to describe the behavior far from the free surfaces. However, the use of axisymmetric perturbations for the oscillatory states appears to cause more serious difficulties. In fact, in this case we observe nonaxisymmetric patterns with angular wave number m [from perturbations in $\exp i(st + qz + m\theta)$] different from zero. An important feature in this kind of system is that noninteger values for m are allowed, in contrast to the classical Taylor-Couette case when propagating nonaxisymmetric structures arise. If we define

$$m = \frac{2\pi \left[\frac{r_o + r_i}{2} \right] \tan\alpha}{d\lambda} , \tag{6}$$

then we find that the experimental value for m is approximately 14 for $\mu = 0$, corresponding to an inclination angle $\alpha = 19°$ and a wavelength $\lambda = 1.22$ (0.86 cm). For $\mu = 0.22$ the experimental value for m is 13.4. We note that the λ we have used is equal to the distance along the axis between successive dark boundaries. We are so far unable to distinguish inflow from outflow boundaries owing to the weak nature of the flows, and this presents us with an ambiguity. The observed boundaries in most cases are equally dark (as determined visually and with image analysis), which is indicative that they may be of the same type, i.e., all inflow or all outflow. In a few cases a set of very weak dark lines can just be detected, apparently revealing that the wavelength is only half that given by the strong dark lines. We are led to the tentative conclusion that either one boundary is much weaker than the other and is thus normally not visible, or that there may exist unobserved weak counter-rotating cells existing next to the inner cylinder. This is a matter that will await resolution in future experiments. It is possible that the value of m may change with both the values of R_i and R_o and the filling volume ratio. Indeed, preliminary experiments[17] have shown that m decreases slightly with a continuous increase of the filling fraction, although the critical Taylor number is unchanged. The Ekman cells induced by the Teflon end rings have a nonaxisymmetric profile and will affect, as a perturbation, the bulk flow. This influence is probably more important near the line $\mu = -1$ (where the velocity gradients are larger) and lower at the line $\mu = 1$. The entry length near the free surfaces, caused by the growth of a boundary layer, may be affecting the inclined rolls since near threshold they are most prominent on only one side, but evidently this is not so important for the Dean or Taylor-Couette rolls.

We emphasize that further transitions have been observed in the system for values of the parameters R_i and R_o beyond the instability thresholds, but they have not yet been quantitatively characterized.

VI. CONCLUSION

We have shown that the flow between two horizontal coaxial rotating cylinders with a partially filled gap is very rich in nonequilibrium patterns. We have found a variety of different structures extending over wide ranges of the external control parameters R_o and R_i. Five primary instability branches and four codimension-2 points have been directly observed. Approximate characteristics of the states (threshold control parameter values, frequency of inclined rolls at threshold, and wavelengths) have been determined. However, our results indicate the need for further, more extensive, investigations. Theoretically, account must be taken of nonaxisymmetric perturbations, a finite gap, and nonlinearities. The last is no doubt important in the vicinity of the codimension-2 points, where mixed-mode patterns have been observed. It may also be important to explore the effect of radius ratio changes. Experimentally it would be desirable to establish the details of the flows in the codimension-2 point neighborhoods,[18] search for possible changes in tilt and propagation velocity of the inclined rolls as functions of R_o and R_i,[19] and explore the behavior of the various flows as the system is driven beyond threshold into chaotic or weakly turbulent states. The last is potentially quite interesting since this system breaks the rotational symmetry of the circular Couette flow, thus undoubtedly changing the dynamics in a profound way, even for the flows bifurcating from the Taylor-like rolls.

ACKNOWLEDGMENTS

We would particularly like to thank Diane Jacobs for her help in programming and Kalliroscope management. I.M. wishes to thank all the staff of the Nonlinear Dynamics Laboratory of the Department of Physics of the Ohio State University for all that they did to make his stay pleasant. We also express our gratitude to Christiane Normand for assistance in checking numerical results. This work was supported in part by the Office of Naval Research under Contract No. N00014-86-K0071 and the French Ministry of Cooperation (CIES) which supported the travel expenses of I.M.

---

*Permanent address: Laboratoire d'Hydrodynamique et Mecanique Physique, Ecole Supérieure de Physique et de Chimie Industrielles de la Ville de Paris, 10 rue Vauquelin, 75231 Paris Cédex 05, France.

[1]S. Chandrasekhar, *Hydrodynamic and Hydromagnetic Stability* (Oxford University, London, 1961), Chaps. VII and VIII.

[2]P. G. Drazin and W. H. Reid, *Hydrodynamic Stability* (Cambridge University, Cambridge, 1981), Chap. 3.

[3]R. C. DiPrima and H. L. Swinney, in *Hydrodynamic Instabilities and the Transition to Turbulence,* Vol. 45 of *Topics in Applied Physics,* edited by H. L. Swinney and J. P. Gollub (Springer, New York, 1981), Chap. 6.

[4]C. D. Andereck, S. S. Liu, and H. L. Swinney, J. Fluid Mech. **164**, 155 (1986).

[5]H. Peerhossaini, Thèse de Doctorat et Sciences, Université de Paris VI, 1987.

[6]W. R. Dean, Proc. R. Soc. London, Ser. A **121**, 402 (1928).

[7]I. Mutabazi, H. Peerhossaini, and J. E. Wesfreid, in *Propagation in Systems Far From Equilibrium, Proceedings in Physics,* edited by J. E. Wesfried and H. R. Brand (Springer, New York, in press).

[8]D. B. Brewster and A. H. Nissan, Chem. Eng. Sci. **7**, 215 (1958).

[9]D. B. Brewster, P. Grosberg, and A. H. Nissan, Proc. R. Soc. London, Ser. A **251**, 76 (1959).

[10]R. C. DiPrima, J. Fluid. Mech. **6**, 462 (1959).

[11]T. H. Hughes and W. H. Reid, Z. Angew. Math. Phys. **7**, 573 (1964).

[12]D. C. Raney and T. S. Chang, Z. Angew. Math. Phys. **22**, 680 (1971).

[13]I. Mutabazi, H. Peerhossaini, J. E. Wesfreid, and C. D. Andereck (unpublished).

[14]I. Mutabazi, C. Normand, H. Peerhossaini, and J. E. Wesfreid (unpublished).

[15]G. W. Baxter and C. D. Andereck, Phys. Rev. Lett. **57**, 3046 (1986).

[16]S. Chandrasekhar, *Hydrodynamic and Hydromagnetic Stability* (Oxford University, London, 1961), pp. 350–359.

[17]Experiments performed at the Weizmann Institute, Rehovot (Israel) [J. E. Wesfreid (personal communication)].

[18]G. Iooss, in *Trends in Applications of Pure Mathematics to Mechanics,* Vol. 249 of *Lecture Notes in Physics,* edited by E. Kröner and K. Kirchgässner (Springer-Verlag, Berlin, 1986), p. 297.

[19]W. F. Langford, R. Tagg, E. J. Kostelich, H. L. Swinney, and M. Golubitsky, Phys. Fluids **31**, 776 (1988).

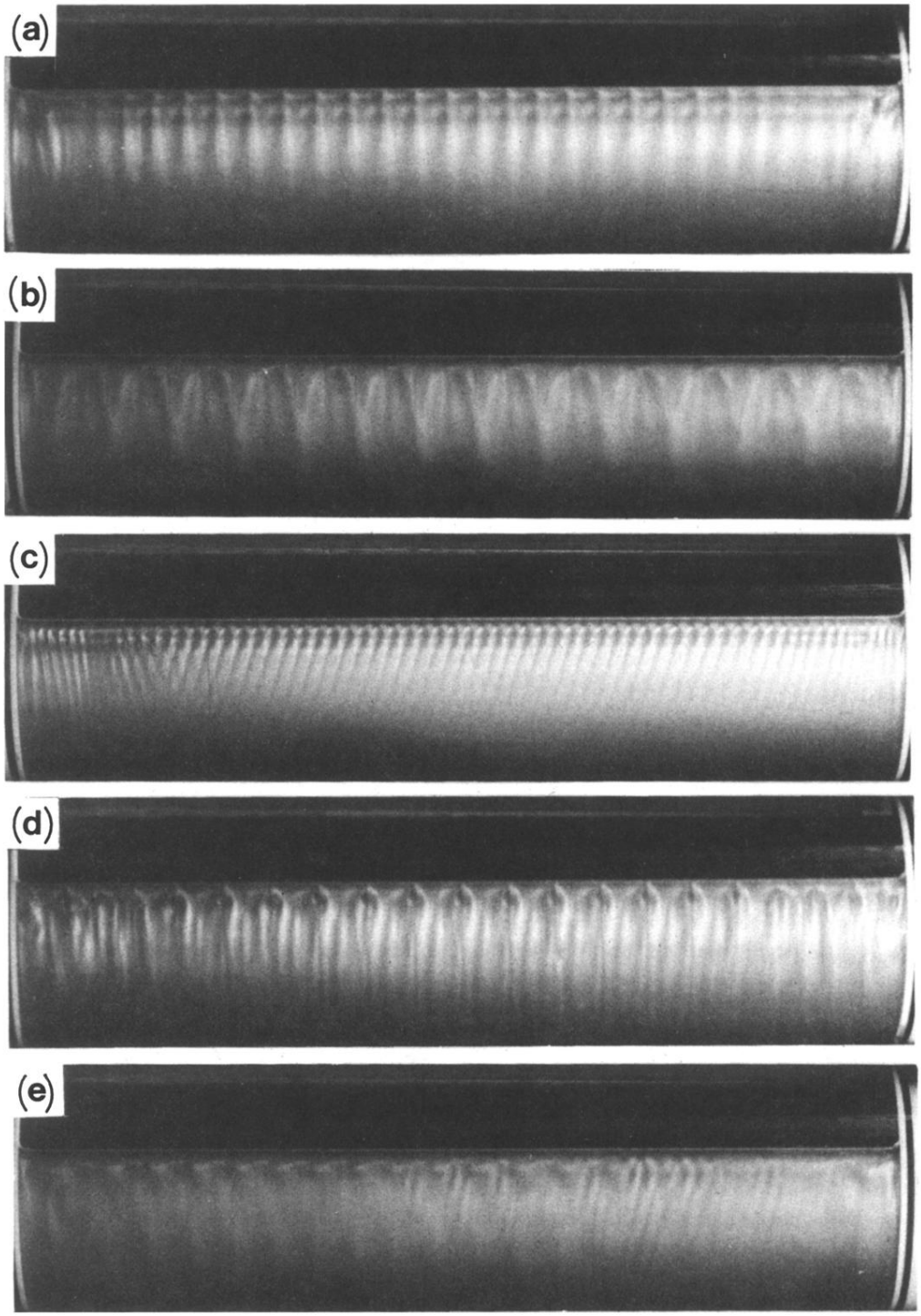

FIG. 4. States observed for different values of control parameters: (a) Dean rolls, $R_o = 220$, $R_i = 195$, (b) Taylor-Couette rolls, $R_o = -136$, $R_i = 252$, (c) inclined traveling rolls, $R_o = 70$, $R_i = 280$, (d) Dean rolls for only the outer cylinder rotating, $R_o = 320$, $R_i = 0$, (e) coexisting inclined and Dean rolls, $R_o = -45$, $R_i = 265$.